

# Supplementary Information

## **Influence of polymer architecture, ionization, and salt annealing on the stiffness of weak polyelectrolyte multilayers**

Jordan Brito,<sup>a</sup> Annie Luse,<sup>b</sup> Aliaksei Aliakseyeu,<sup>c</sup> and Svetlana A. Sukhishvili<sup>a\*</sup>

- a. Department of Materials Science & Engineering, Texas A&M University, College Station, Texas 77843, USA.
- b. Department of Physics and Astronomy, Texas A&M University, College Station, Texas 77843, USA.
- c. Artie McFerrin Department of Chemical Engineering, Texas A&M University, College Station, Texas 77843, USA.

### **Procedure for measuring the buckling wavelength $\lambda$ from images using ImageJ:**

From the raw image, first the scale of the image is set by drawing a straight line across the diameter of the field of view and setting the line length equal to 2666.7  $\mu\text{m}$ . Then, the brightness and contrast of the image was adjusted to enhance the wrinkles. Using the Line Profile tool, a line was drawn perpendicular to a set of wrinkles, typically near a crack where the wrinkles are most uniform. Using the Plot Profile tool, a plot of the grayscale values across the lines are plotted along the length of the line. The Find Peaks script from BAR was used to find the positions of the minima and maxima, excluding the peaks on the edge of the plot. The x-values of the maxima or minima were sorted from smallest to largest, and the distance between each was calculated using  $x_{i+1} - x_i$ . These distance between each extreme were averaged and identified as the buckling wavelength,  $\lambda$ .

Citation for BAR scripts:

Ferreira, T., Miura, K., Chef, B., & Eglinger, J. (2015). Scripts: BAR 1.1.6 (Version 1.1.6). Zenodo. [doi:10.5281/ZENODO.28838](https://doi.org/10.5281/ZENODO.28838)

**Propagation of error analysis for the Young's modulus of the PEM film,  $E_f$ :**

$$\Delta E_f = \sqrt{\left(\frac{\partial E_f}{\partial \lambda}\right)^2 \Delta \lambda^2 + \left(\frac{\partial E_f}{\partial d_f}\right)^2 \Delta d_f^2}$$

where  $E_f = \frac{3E_s(1-v_f^2)}{1-v_s^2} \left(\frac{\lambda}{2\pi d_f}\right)^3$ ,  $\Delta \lambda$  is the standard deviation of the buckling wavelength, and  $\Delta d_f$  is the standard deviation of the PEM film thickness.

Now, assuming that  $\frac{3E_s(1-v_f^2)}{1-v_s^2}$  is a constant, now denoted  $c_1$ ,

$$\Delta E_f = \sqrt{\left(\frac{3c_1\lambda^2}{(2\pi d_f)^3}\right)^2 * \Delta \lambda^2 + \left(\frac{-3c_1\lambda^3}{(2\pi)^3 d_f^4}\right)^2 * \Delta d_f^2}$$

Factoring out values to simplify this equation yields:

$$\Delta E_f = \sqrt{\frac{9c_1^2\lambda^4}{d_f^6(2\pi)^6} \left( \Delta \lambda^2 + \left(\frac{\lambda}{d_f}\right)^2 * \Delta d_f^2 \right)}$$

Further simplification of this equation yields:

$$\Delta E_f = \frac{3\lambda^2 c_1}{8\pi^3 d_f^4} \sqrt{(d_f^2 \Delta \lambda^2 + \lambda^2 \Delta d_f^2)}$$

Please note that the  $d_f$  values have units of nanometers ( $10^{-9}$  m) and the  $\lambda$  values have units of micrometers ( $10^{-6}$  m), so the influence of the  $\lambda$  error is more significant in these error calculations. Because of the constant (*i.e.*, not varying between image) pixel-limited resolution of the image analyses, we have limited the minimum error to 0.44  $\mu$ m for all images.

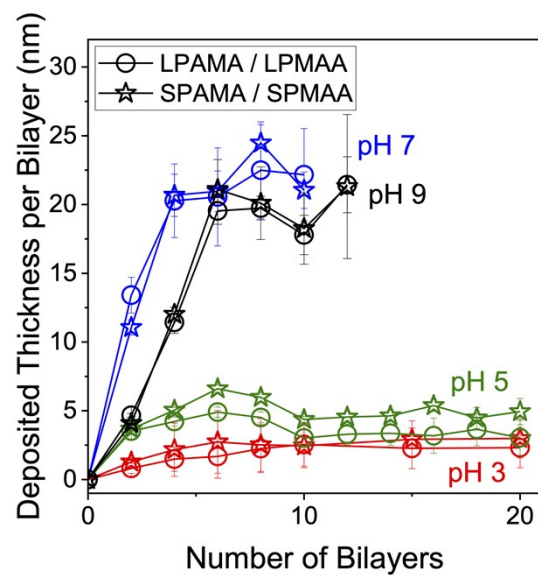


**Figure S1.** Deposited thickness per bilayer for LPAMA / LPMAA and SPAMA / SPMAA polyelectrolyte multilayers (PEMs) assembled from solutions at pH 3, 5, 7, and 9, as measured by spectroscopic ellipsometry. Error bars were calculated from four measurements.

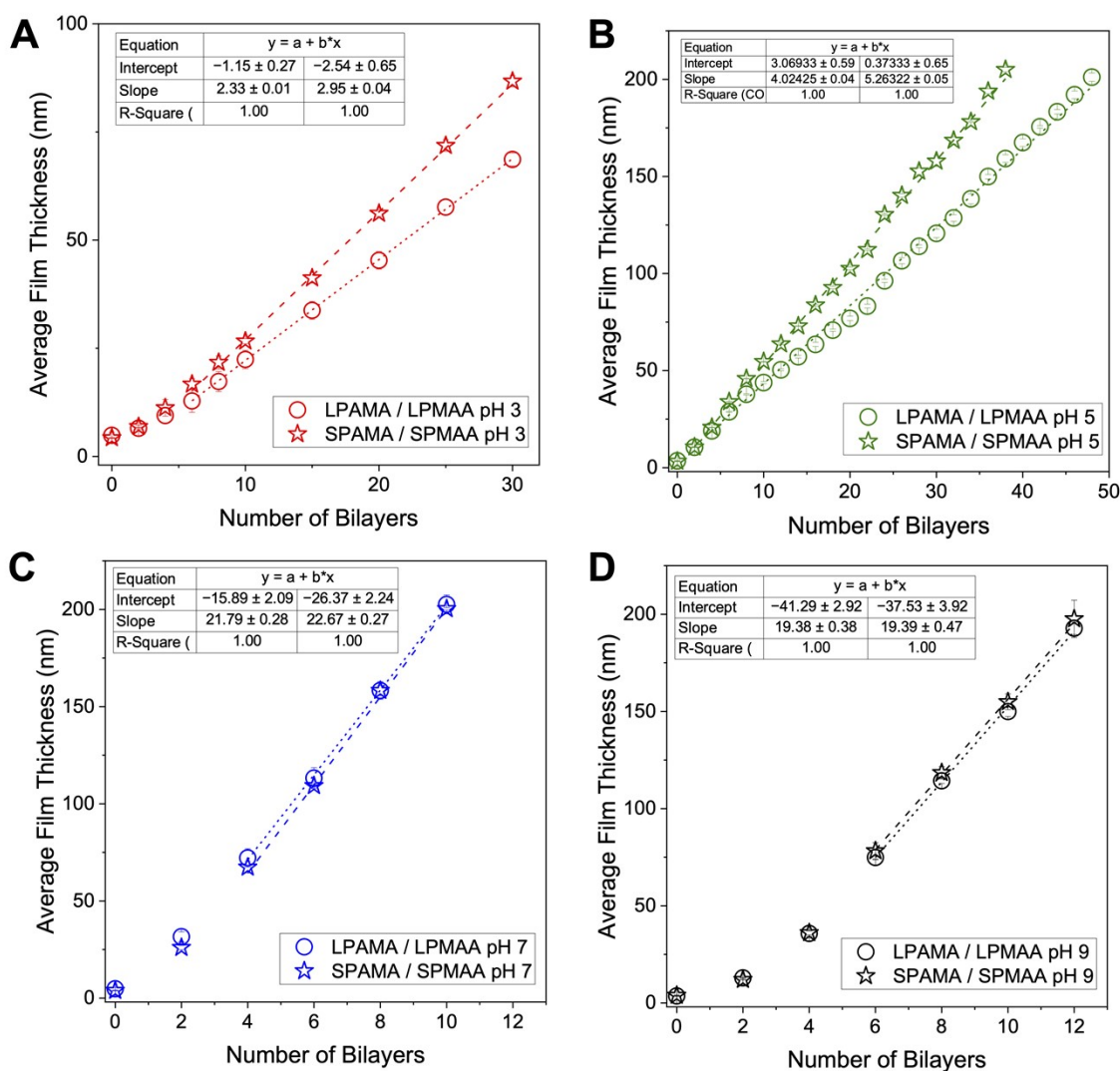


**Figure S2.** Linear trendlines in the linear growth regime for LPAMA / LPMAA and SPAMA / SPMAA polyelectrolyte multilayers (PEMs) assembled from solutions at pH 3, 5, 7, and 9, as measured by spectroscopic ellipsometry. Error bars for each thickness were averaged from four measurements (two different spots on two samples).

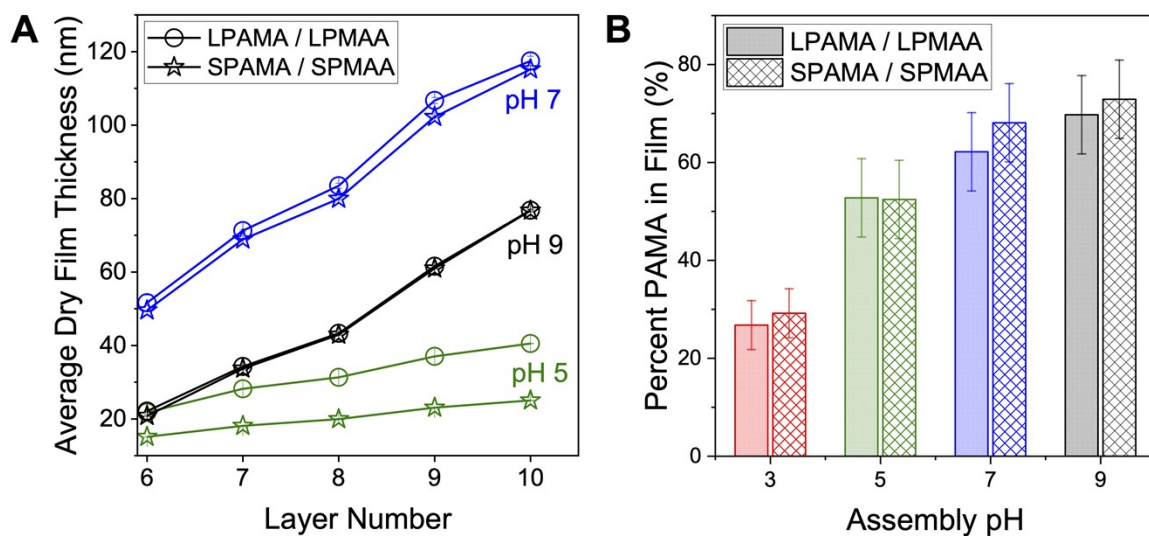


**Figure S3.** (A) Individual layer thickness measurements for LPAMA / LPMAA and SPAMA / SPMAA polyelectrolyte multilayers (PEMs) assembled from solutions at pH 5, 7, and 9, as measured by spectroscopic ellipsometry. PMAA is the top layer at even layer numbers, and PAMA is the top layer at odd layer numbers. Error bars were averaged from six measurements (three different spots on two samples). Discrepancies between growth curves may result from the extra drying steps introduced when collecting single layer measurements. (B) Molar percentage of PAMA in the PEMs assembled from each pH as determined by infrared spectroscopy. Similar trends were calculated from the individual layer ratios in panel A, but with higher error.

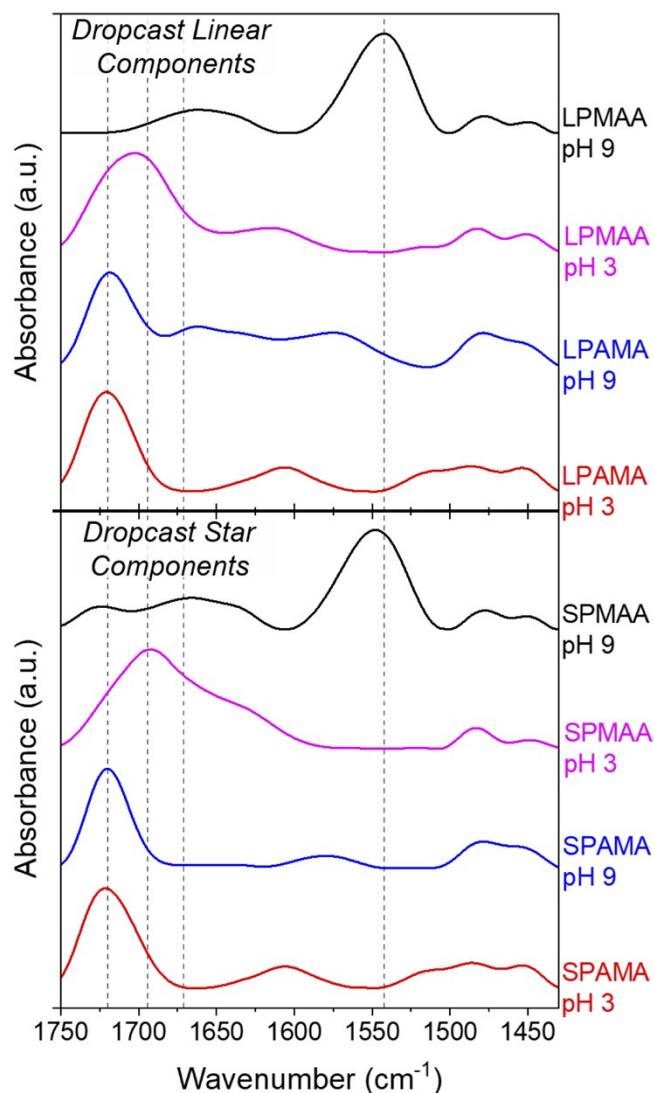


**Figure S4.** Infrared spectra of individual components – LPAMA and LPMAA (A), and SPAMA and SPMAA (B) – with important peaks identified by dotted vertical lines. The line at 1725 cm<sup>-1</sup> corresponds with the carbonyl stretching in PAMA ester group, 1700 cm<sup>-1</sup> with the carbonyl stretching in protonated PMAA carboxylic acid groups, 1670 cm<sup>-1</sup> with the hydrogen-bonded dimers of carboxylic acid groups in PMAA, and 1550 cm<sup>-1</sup> with the carboxylate stretching in ionized PMAA.

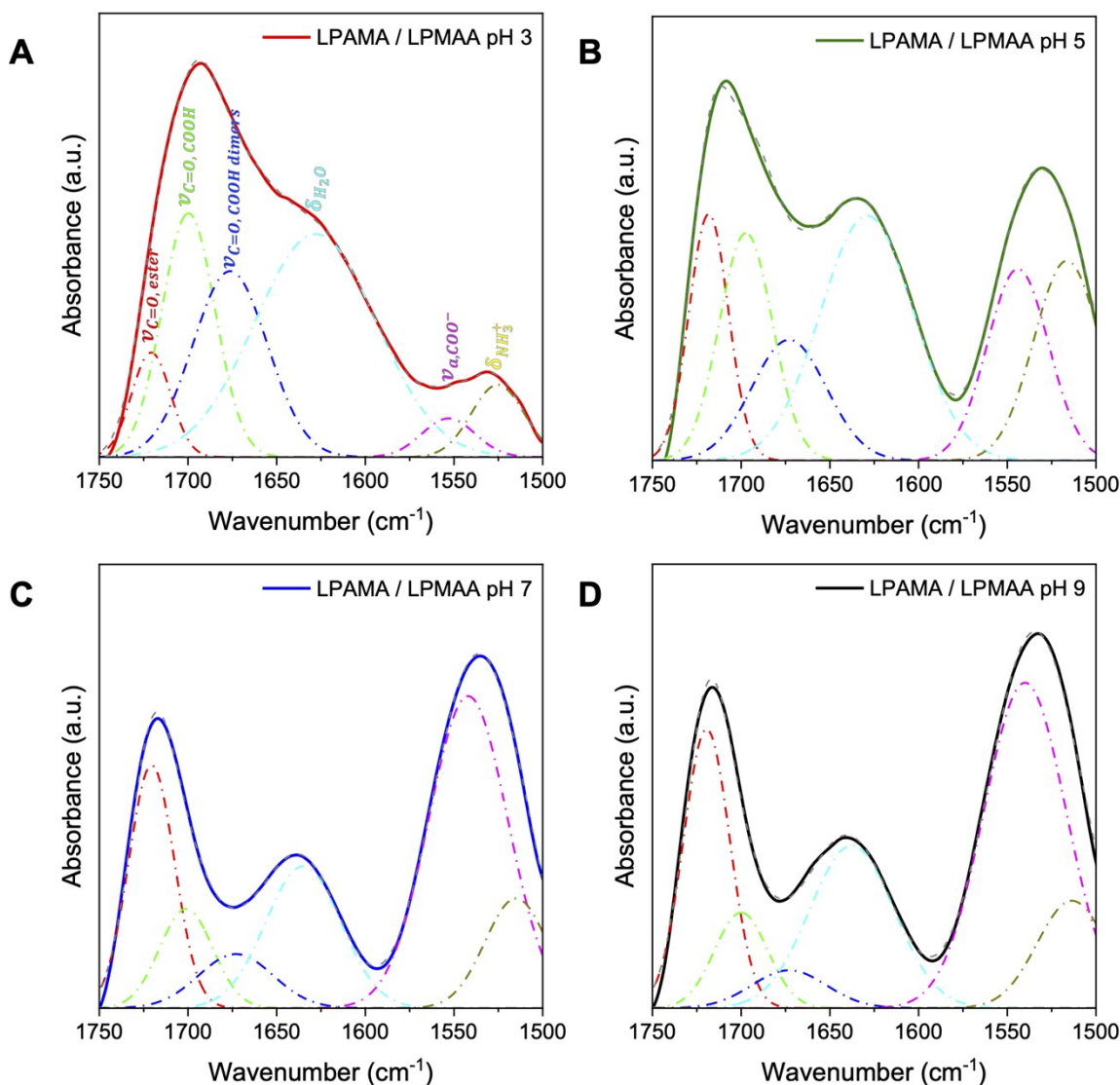


**Figure S5.** Deconvoluted ATR-FTIR spectra of LPAMA / LPMAA multilayer films deposited from pH 3, 5, 7, and 9 solutions, all with LPMAA as the top layer. The real data are plotted with solid bold lines, and fitted curves are with dashed lines. The red curve at  $\sim 1725\text{ cm}^{-1}$  corresponds with the carbonyl stretching in PAMA ester group, the green curve at  $\sim 1700\text{ cm}^{-1}$  corresponds with the carbonyl stretching in protonated PMAA carboxylic acid groups, the blue curve at  $\sim 1670\text{ cm}^{-1}$  corresponds with the hydrogen-bonded dimers of carboxylic acid groups in PMAA, and the magenta curve at  $\sim 1550\text{ cm}^{-1}$  corresponds with the carboxylate stretching in ionized

PMAA. The cyan peak at  $\sim 1640\text{ cm}^{-1}$  and the brown peak at  $\sim 1520\text{ cm}^{-1}$  are likely due to water and amine contributions, respectively.

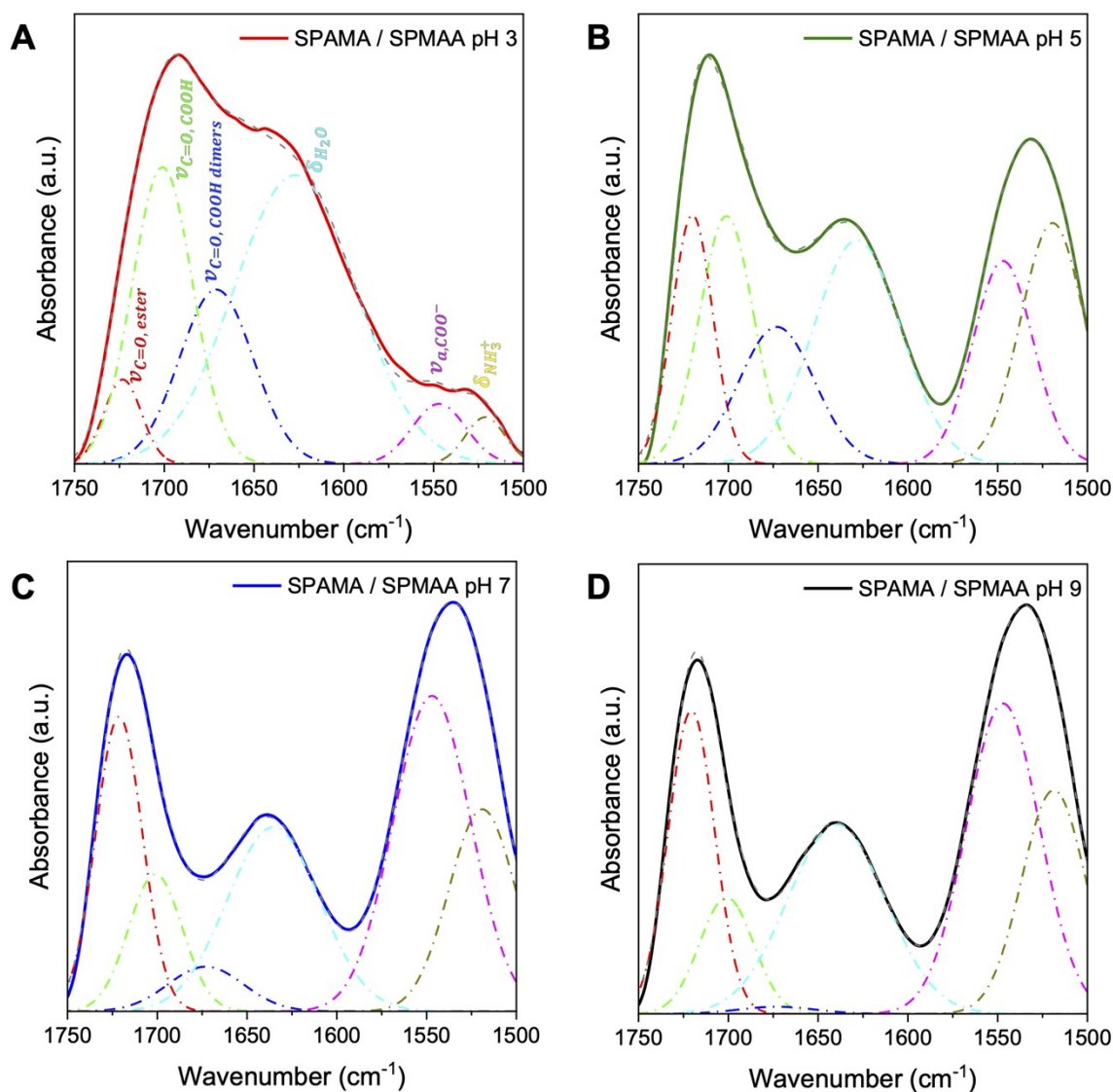


**Figure S6.** Deconvoluted ATR-FTIR spectra of SPAMA / SPMAA multilayer films deposited from pH 3, 5, 7, and 9 solutions, all with SPMAA as the top layer. The real data are plotted with solid bold lines, and fitted curves are with dashed lines. The red curve at  $\sim 1725\text{ cm}^{-1}$  corresponds with the carbonyl stretching in PAMA ester group, the green curve at  $\sim 1700\text{ cm}^{-1}$  corresponds with the carbonyl stretching in protonated PMAA carboxylic acid groups, the blue curve at



$\sim 1670\text{ cm}^{-1}$  corresponds with the hydrogen-bonded dimers of carboxylic acid groups in PMAA, and the magenta curve at  $\sim 1550\text{ cm}^{-1}$  corresponds with the carboxylate stretching in ionized PMAA. The cyan peak at  $\sim 1640\text{ cm}^{-1}$  and the brown peak at  $\sim 1520\text{ cm}^{-1}$  are likely due to water and amine contributions, respectively.

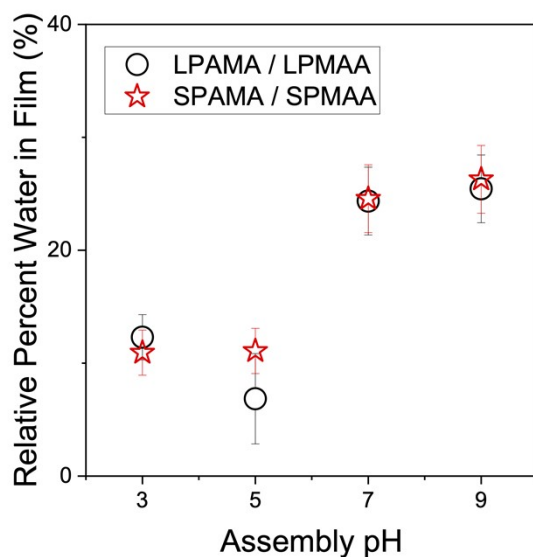


**Figure S7.** Relative water content of LPAMA / LPMAA (circle symbols) and SPAMA / SPMAA (star symbols) PEM films deposited from pH 3, 5, 7, and 9.

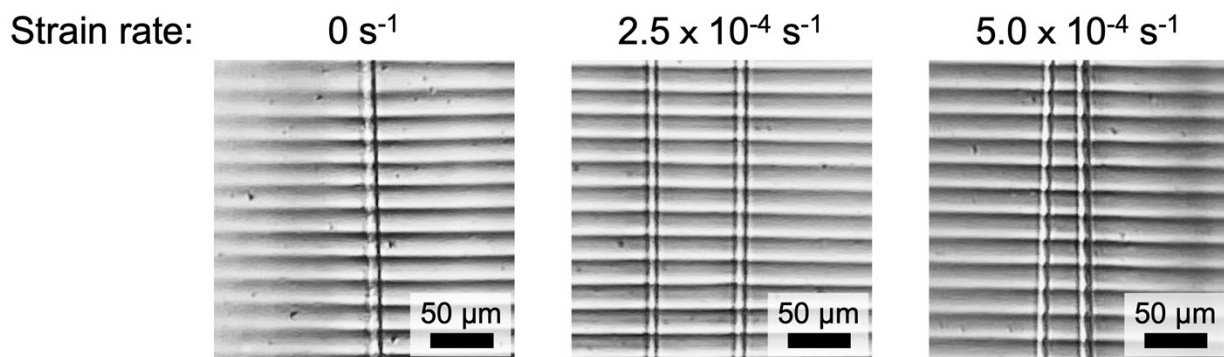


**Figure S8.** Optical images demonstrating the lack of effect of strain rate on the buckling wavelength, in this case for LPAMA / LPMAA assembled at pH 7.

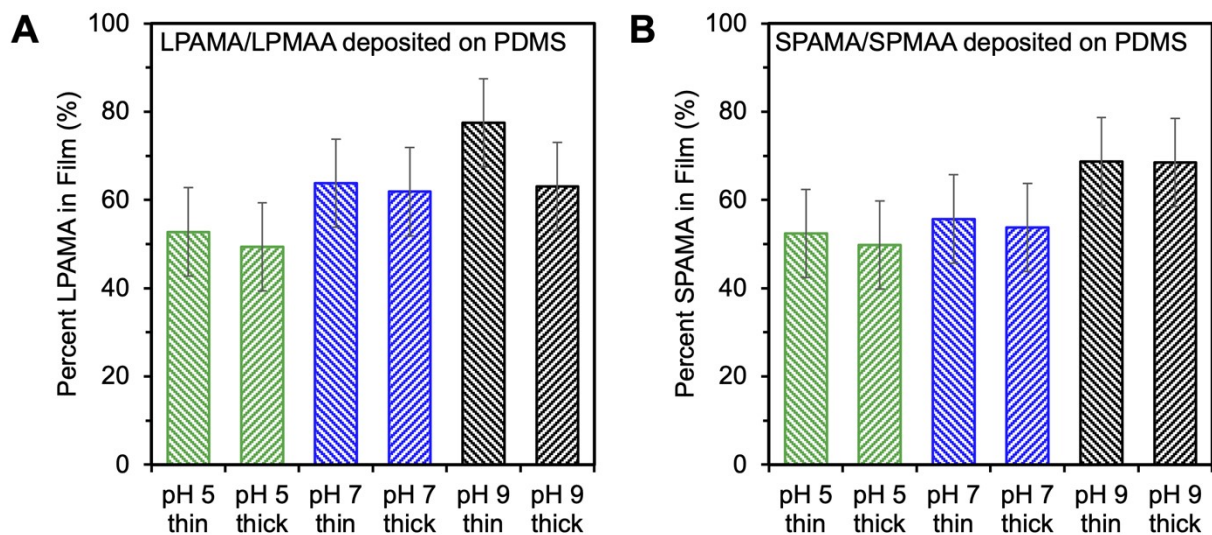


**Figure S9.** Thickness dependence of the molar percent of LPAMA (A) and SPAMA (B) in PEMs deposited on PDMS from solutions at pH 5, 7, and 9, as determined by infrared analysis. ‘Thin’ films and ‘thick’ films have an average dry film thickness of ~150 nm and ~350 nm, respectively, as determined by spectroscopic ellipsometry.

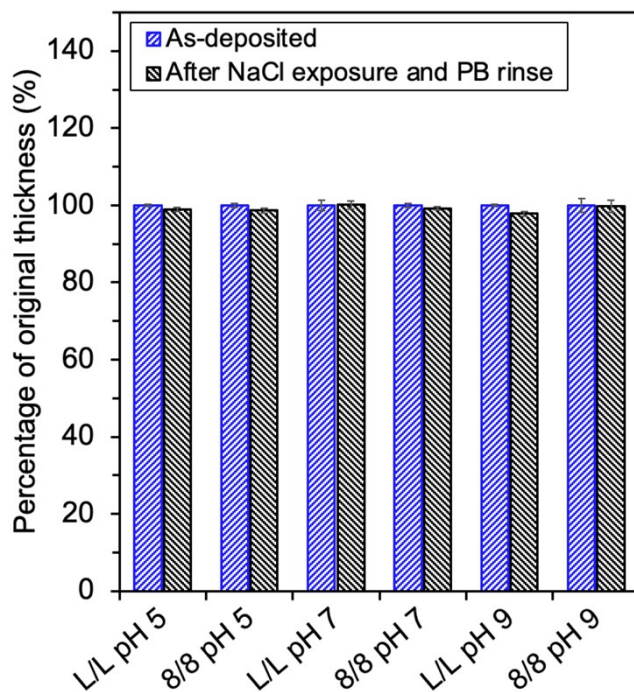


**Figure S10.** Change in thickness of LPAMA / LPMAA (denoted ‘L/L’) and SPAMA / SPMAA (denoted ‘8/8’) PEM films deposited from pH 5, 7, and 9 solutions before and after being

exposed to 0.5 M NaCl solutions at matched pH for 30 min, rinsed in 0.01 phosphate buffer at matched pH, and dried under a flow of nitrogen gas.

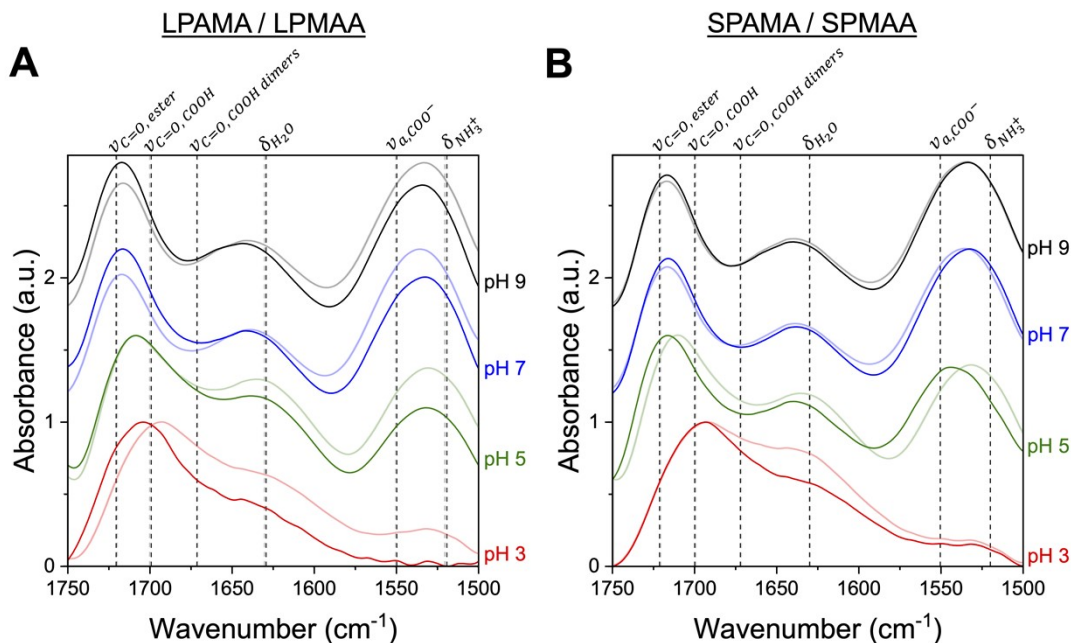


**Figure S11.** Infrared spectra of LPAMA / LPMAA (A) and SPAMA / SPMAA (B) multilayer films deposited from pH 3, 5, 7, and 9 solutions before (faded spectra) and after being exposed to 0.5 M NaCl solutions at matched pH for 30 min, rinsed in 0.01 phosphate buffer at matched pH, and dried under a flow of nitrogen gas (bold spectra).

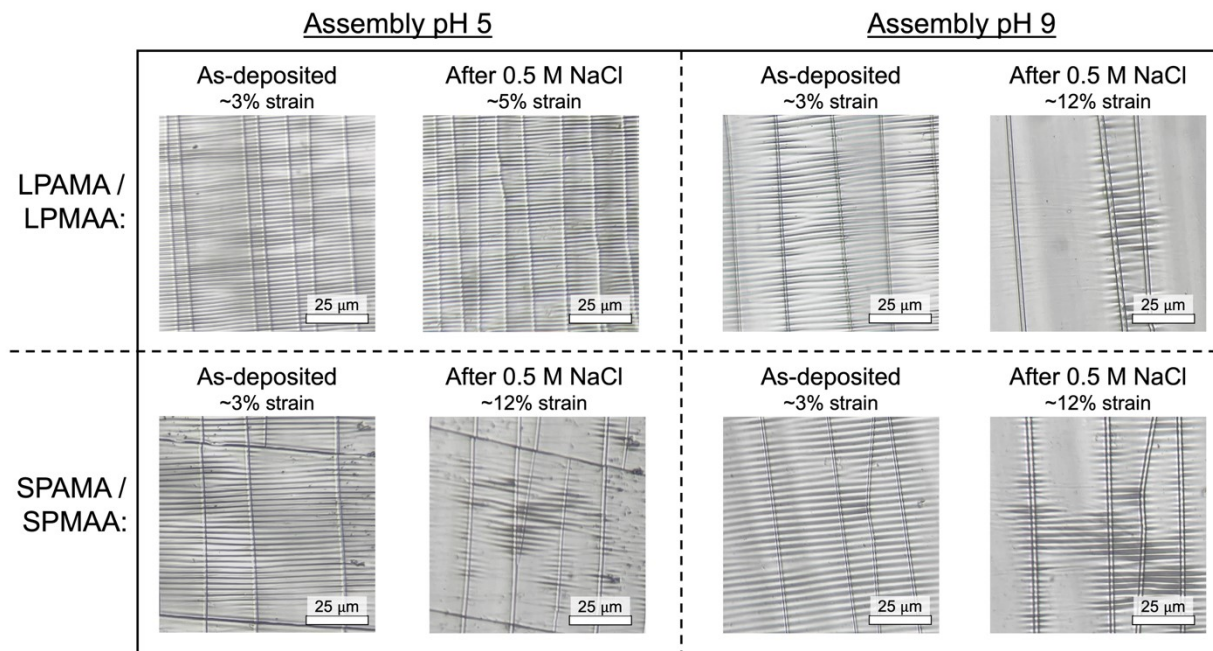


**Figure S12.** Optical images of cracking and wrinkling of LPAMA / LPMAA (top row) and SPAMA / SPMAA films (bottom row) assembled from solutions at pH 5 and 9. Images were collected from films at their critical wrinkle strain as-deposited and after salt-annealing at 0.5 M NaCl for 30 min and rinsing in phosphate buffer at the same pH as assembly. All scale bars are 25  $\mu\text{m}$ .

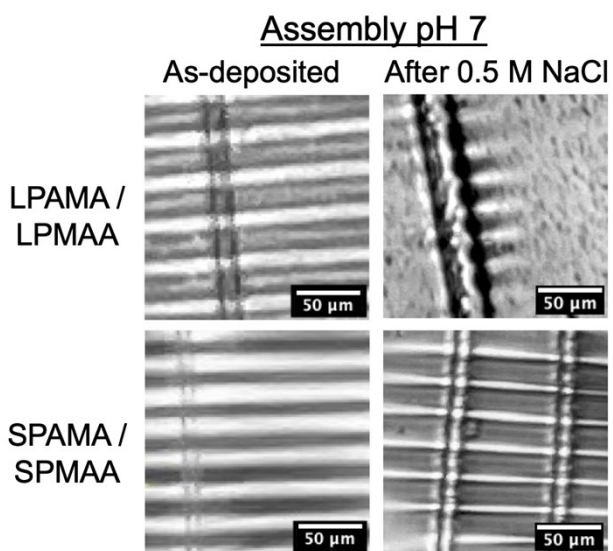


**Figure S13.** Optical images of cracking and wrinkling of LPAMA / LPMAA (top row) and SPAMA / SPMAA films (bottom row) assembled from solutions at pH 7. Images were collected

from films at their critical wrinkle strain as-deposited and after salt-annealing at 0.5 M NaCl for 30 min and rinsing in phosphate buffer at the same pH as assembly. All scale bars are 50  $\mu\text{m}$ .